What will next-generation X-ray observatories do for the large scale jets of quasars?

The first hard X-ray spectrum of a kpc-scale jet with NuSTAR

Markos Georganopoulos[1,2], Eileen Meyer[1], Aamil Shaik[1]

[1]University of Maryland Baltimore County, Baltimore, MD USA. [2]NASA Goddard Space Flight Center, Greenbelt, MD USA

Summary: High-resolution imaging with Chandra and HST has revealed that many powerful jets emit strongly in the optical/UV and X-rays on kpc to Mpc scales. In the most powerful jets, the optical and X-ray have spectral properties which show they are not a continuation of the radio synchrotron emission. These extra high-energy emission components, despite dominating the energetic output, are currently unidentified. Understanding the emission mechanism in jets is the only way to get a proper accounting of the energy they carry and the impact on their environments. **We present a deep (350 ks) NuSTAR observation of Pictor A, the only large-scale resolved jet target which can be easily resolved and detected separately from the AGN core.** We find that the combined Chandra + NuSTAR X-ray spectrum, after an initial softening spectral break at ~ 2 keV, hardens again at ~ 7 keV, with no sign of a high-energy cut-off. The total X-ray spectrum thus suggests two spectral components. We confirm strong variability in the hotspot as seen by Chandra, and some hints of the same in the NuSTAR observations. We interpret the full suite of observations as indicating a synchrotron origin for the X-ray emission, from a distinct electron energy distribution from that which produces the radio emission.

NuSTAR Observations

Project, PI	Date	Exp (s)	Filt. Exp(s)
Wilson	2015 Dec 3	109.5	92.82
Meyer	2021 Nov 28	126.2	104.1
	2021 Dec 01	37.59	32.39
	2021 Dec 02	138.8	118.6
TOTAL:		412.1	347.9

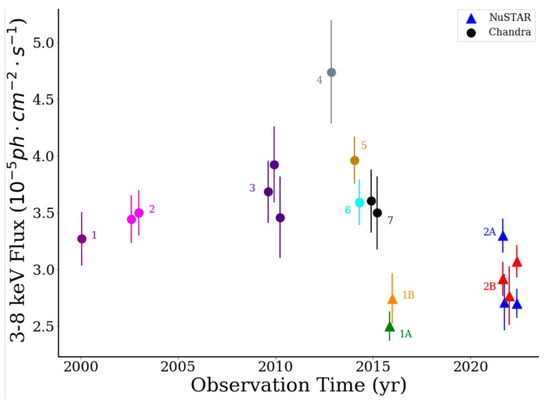

After filtering, the combined NuSTAR exposure was 350 ks. We also reduced and analyzed 330 ks of archival Chandra observations of Pictor A (see Reddy et al., 2023 and Meyer et al., 2023 for details). Background modeling for the NuSTAR observations was conducted using the **nuskybgd** IDL script (Wik et al., 2014). The included model components are shown at left (from Wik et al., 2014) and the actual fit to Chandra + NuSTAR observations shown below.

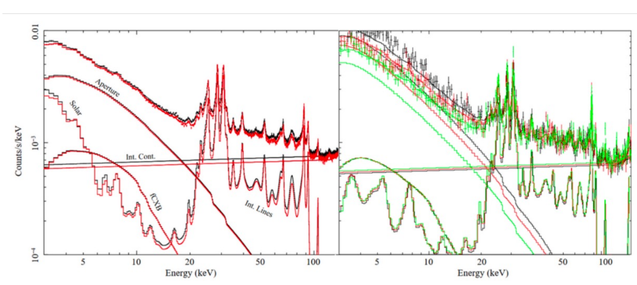

Figure 2. Background model components included in nuskybgd. The code fits background counts extracted from multiple annular regions with negligible source emission. The spectral fits for these different annuli are depicted as the red, green, and black spectra. The simultaneous fit constrains the spectral parameters and map the spatial variations of the background across the detector.

Figure 3. Below left, the results of the combined fit of Chandra and NuSTAR observations (all epochs). In upper panel the solid line plots the flux of the best-fit broken power law model which is favored by the Bayesian evidence and the shaded contours around either line displays the 2σ range of the posterior distribution. Lower panel, residuals of the best-fit power law model and posterior distribution as compared to the spectral data.

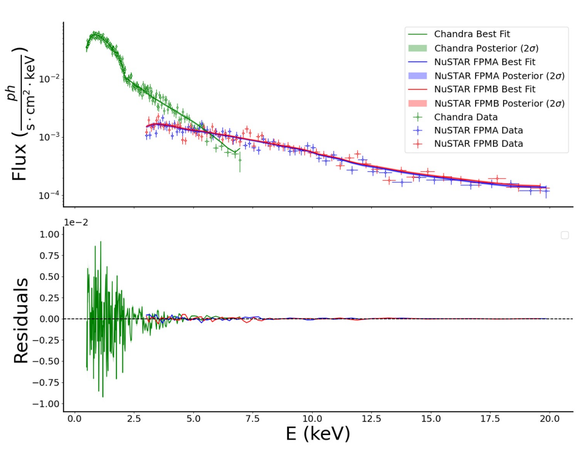

Table 3. The AIC, BIC, the Bayesian evidence normalized to the most probable model, and the relative probabilities of each model for the combined Chandra + NuSTAR fit. In contrast to the analyses of the NuSTAR and Chandra data separately, to the Bayesian evidence of the combined data overwhelmingly favors the double broken power law model.

Model	ΔBIC	ΔAIC	$\log(Z)$	$p(M\|D)$
bkn2pow	-1183	-1200	0.0	1
zbknpower	-1155	-1171	-7.1	0
zlogpar	-1143	-1152	-10.9	0
zpowerlw	-1139	-1139	-12.5	0
zcutoffpl	-1103	-1111	-19.3	0
apec	0.0	0.0	-260.0	0

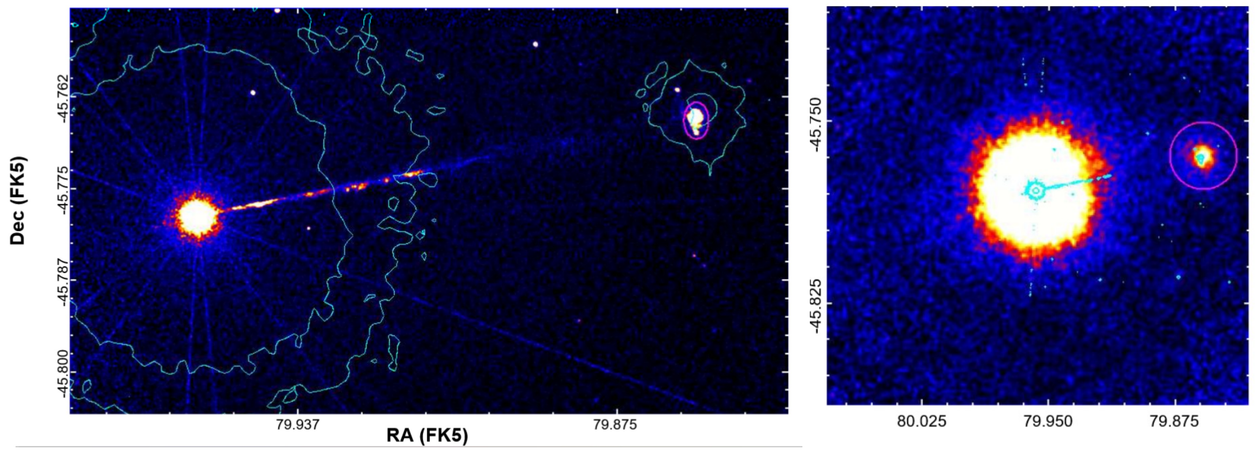

Figure 1. Combined Deep Chandra ACIS image of Pictor A, with contours from combined NuSTAR observation overlaid.

Spectral Fitting and SED

The broad-band SED of the Pictor A hotspot includes, for the first time, data for the hard X-rays up to 20 keV (beyond which the source is not detected by NuSTAR due to low statistics). The Chandra observations alone confirm a broken power law with a softening spectral break at ~3.2 keV, from Γ =1.98 ± 0.02 —> 3.25 ± 0.16. The combined NuSTAR observations are best fit with a single powerlaw of Γ =1.0 ± 0.12, with no sign of a cut-off. This requires a substantial hardening if the change is not due to variability. The NuSTAR normalization factor was 0.55 during the joint fit, a larger discrepancy than expected which suggests variability between the NuSTAR and Chandra observations.

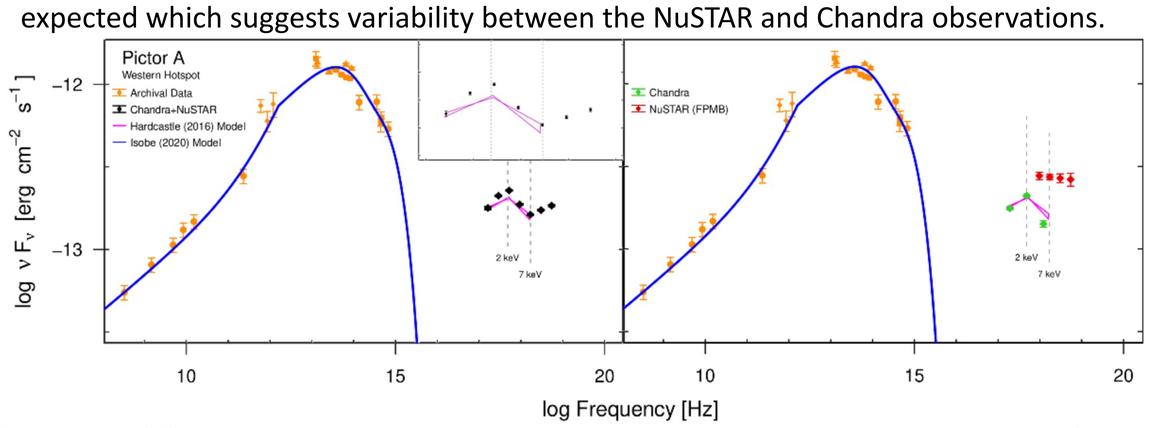

Figure 4. Hotspot SED. Archival radio – optical data is consistent with a synchrotron spectrum, modeled as a broken cutoff powerlaw (Isobe et al., 2017). At left, the combined Chandra+NuSTAR fit, forcing consistency in the overlapping range. At right, the individual fits to the Chandra and NuSTAR observations, which suggest variability.

Gamma-ray upper limits (not shown, Shaik et al., in prep.) as well as jet/counter-jet ratio (Hardcastle et al., 2016) and X-ray variability of the hotspot rule out an IC/CMB origin for the X-ray emission of the hotspot. Synchrotron emission from a second population of electrons explanation for the X-rays. The observations presented here suggest multiple components in the X-ray spectrum, or strong spectral variability.

Table 3. Model Fit Results for combined Chandra + NuSTAR spectral fit. The preferred model for the entire range is the double broken power law, in comparison with the single-broken power law preferred for the Chandra and NuSTAR data sets individually.

Power Law	Broken PL	Cutoff PL	Thermal	Log-Parabola	Double Broken PL
$N_1 = 25.3^{+0.4}_{-0.4}$	$N_1 = 26.4^{+0.4}_{-0.5}$	$N_1 = 26.8^{+0.4}_{-0.4}$	$N_1 = 43.5^{+0.5}_{-0.5}$	$N_1 = 25.9^{+0.5}_{-0.4}$	$N_1 = 26.3^{+0.4}_{-0.5}$
$\Gamma = 2.07^{+0.01}_{-0.01}$	$\Gamma_1 = 1.96^{+0.03}_{-0.03}$	$\Gamma = 1.95^{+0.01}_{-0.01}$	$kT = 3.94^{+0.07}_{-0.07}$	$\alpha = 2.02^{+0.02}_{-0.02}$	$\Gamma_1 = 1.98^{+0.02}_{-0.02}$
	$\Gamma_2 = 2.19^{+0.03}_{-0.03}$	$E_{cut} = 19.69^{+0.23}_{-0.53}$		$\beta = 0.10^{+0.03}_{-0.03}$	$\Gamma_2 = 2.64^{+0.13}_{-0.12}$
	$E_{brk} = 1.69^{+0.24}_{-0.18}$				$\Gamma_3 = 1.94^{+0.05}_{-0.05}$

Variability

X-ray variability has previously been observed in several jet knots of Pictor A using Chandra (Marshall et al., 2010). In the hotspot, Hardcastle et al., (2016) similarly reported quite short-timescale variability, which we also confirm at the 6.7σ level using a novel maximum likelihood test (see Meyer et al., 2023).

Table 4. Results of Maximum-likelihood test for variability on various groupings of Chandra or NuSTAR data. (Note: due to poorly constrained systematic offsets between NuSTAR and Chandra we do not attempt to compare Chandra and NuSTAR epochs for variability). Variability signal appears to increase with time in both cases. Additional NuSTAR epochs are needed to further test for hard X-ray variability.

Observatory	Epoch(s)	P-Value	Significance	Δt
Chandra	1-3	0.064	1.85	9 yr
Chandra	5,6	9.02e-4	3.32	3 mo
Chandra	4-7	3.19e-5	4.16	2 yr
Chandra	All	2.04e-11	6.70	15 yr
NuSTAR	2	0.820	0.23	1 wk
NuSTAR	All	0.082	1.74	6 yr

*See also Poster #003 in section 13 "AGN Jets are X-Ray Variable on kpc Scales"

Contact:

Eileen Meyer | Markos Georganopoulos
University of Maryland Baltimore County
meyer@umbc.edu | georgano@umbc.edu

astro.umbc.edu

References

Reddy, K., Georganopoulos, M., & Meyer, E. T. 2021a, ApJS, 253, 37, doi: 10.3847/1538-4365/abd8d7
Hardcastle, M. J., Lenc, E., Birkinshaw, M., et al. 2016a, MNRAS, 455, 3526, doi: 10.1093/mnras/stv2553
Meyer, E. T., Shaik, A., Georganopoulos M., et al., Nature Astronomy, 29 May 2023
Wik, D. R., Hornstrup, A., Molendi, S., et al. 2014, ApJ, 792, 48, doi: 10.1088/0004-637X/792/1/48
Marshall, H.L., Hardcastle, M.J., Birkinshaw, M., et al. 2010, ApJL 714, L213. doi:10.1088/2041-8205/714/2/L213
Thimmappa, R., Stawarz, L, Marchenko, V., et al. 2020, ApJ, 903, 109. doi:10.3847/1538-4357/abb605